

Chaotic Motions and Transition to Stochasticity in the Classical Problem of the Heavy Rigid Body with a Fixed Point.

L. GALGANI and A. GIORGILLI

Istituto di Fisica dell'Università - Milano, Italia

Istituto di Matematica dell'Università - Milano, Italia

J.-M. STRELCYN

Département de Mathématiques, Centre Scientifique et Polytechnique

Université de Paris-Nord - 93430 Villetaneuse, France

(ricevuto il 5 Agosto 1980)

Summary. — We give numerical evidence for the existence of chaotic motions and of a transition to stochasticity in the classical problem of a heavy rigid body with a fixed point, by studying a perturbation of the Euler-Poinsot case. This gives also numerical evidence for the non-integrability of this problem.

1. — Introduction.

Let us consider the classical problem of the motion of a rigid body with a fixed point under the action of a uniform gravity field⁽¹⁻³⁾. In the absence

(1) F. KLEIN and A. SOMMERFELD: *Über die Theorie des Kreisels*, Vol. 1-4 (Leipzig, 1897-1910; New York, N. Y., 1965).

(2) A. GRAY: *A Treatise on Gyrostatics and Rotational Motions* (London, 1918; New York, N. Y., 1959).

(3) T. LEVI CIVITA and U. AMALDI: *Lezioni di meccanica razionale*, Vol. 2, parte 2 (Bologna, 1952).

(4) E. T. WHITTAKER: *A Treatise on the Analytical Dynamics of Particles and Rigid Bodies*, 4th edition (Cambridge, 1959).

(5) V. V. GOLUBEV: *Lectures on Integration of the Equations of Motion of a Rigid Body*

of gravity, or equivalently when the centre of mass coincides with the fixed point (Euler-Poinsot case), the system is well known to be integrable, as two independent integrals of motion in involution (*i.e.* with vanishing mutual Poisson bracket) exist in addition to energy.

In the presence of gravity, one always has a second independent integral, namely the vertical component of the angular momentum, in addition to energy, and the system would be integrable if there were a third independent integral in involution with the second one. Now, apart from the Euler-Poinsot case, the only known integrable cases are those of Lagrange-Poisson and of Kovalevskaja, and it was proven by HUSSON⁽¹⁰⁾ (see also ref. (5,8)) that these cases are the only ones for which the Euler-Poisson equations are integrable by means of algebraic functions. By quoting LEIMANIS⁽⁶⁾, « although the literature on the motion of a heavy rigid body about a fixed point has grown very extensively during the last 65 years, it is concerned almost entirely with consideration of special cases. In conclusion, we note that Klein's and Sommerfeld's hopes that "by finding enough special cases we may some day be able to know more about the general solution of the problem" have not yet come true ».

Indeed, as ARNOL'D says⁽⁹⁾, « the problem of the motion of the heavy rigid body has not been solved and is in some sense unsolvable ».

On the other hand, in the last 25 years, after the fundamental work of Kolmogorov^(11,12), some substantial progress has been obtained in the understanding of small perturbations of integrable systems⁽¹³⁻¹⁷⁾ (see also ap-

about a Fixed Point (Moscow, 1953, in Russian); English translation by the Israel Program of Scient. Transl. (Jerusalem, 1960).

⁽⁶⁾ E. LEIMANIS: *Some recent advances in the dynamics of rigid bodies and celestial mechanics*, in *Surveys in Applied Mathematics*, Vol. 2 (New York, N. Y., 1958), p. 1.

⁽⁷⁾ E. LEIMANIS: *The General Problem of the Motion of Coupled Rigid Bodies about a Fixed Point* (Berlin, 1965).

⁽⁸⁾ JU. A. ARHANGELSKIJ: *The Analytical Dynamics of Rigid Bodies* (Moscow, 1977, in Russian).

⁽⁹⁾ V. I. ARNOL'D: *Mathematical Methods in Classical Mechanics*, grad. texts in Math. No. 60 (Berlin, 1978).

⁽¹⁰⁾ E. HUSSON: *Ann. Fac. Sci. Univ. Toulouse Sci. Math. Sci. Phys.*, **8**, ser. 2, 73 (1906); *Acta Math.*, **31**, 71 (1908).

⁽¹¹⁾ A. N. KOLMOGOROV: *The general theory of dynamical systems and classical mechanics*, in *Proceedings of the 1954 International Congress on Mathematics* (Amsterdam, 1954, in Russian), p. 315 (English translation in R. ABRAHAM and J. E. MARSDEN, *Foundations of Mechanics* (New York, N. Y., 1978)).

⁽¹²⁾ A. N. KOLMOGOROV: *Dokl. Akad. Nauk. SSSR*, **98**, No. 4, 527 (1954 in Russian).

⁽¹³⁾ V. I. ARNOL'D: *Usp. Mat. Nauk. SSSR*, **18**, No. 5, 13 (1963, in Russian) (English translation *Russian Math. Surv.*, **18**, No. 5, 9 (1963)).

⁽¹⁴⁾ V. I. ARNOL'D: *Usp. Mat. Nauk SSSR*, **18**, No. 6, 91 (1963, in Russian) (English translation *Russian Math. Surv.*, **18**, No. 6, 85 (1963)).

⁽¹⁵⁾ J. MOSER: *Stable and random motions in dynamical systems*, in *Annals of Mathe-*

pendix 8 of ref. (9)). Indeed the qualitative property which has been established for systems which are (Hamiltonian, conservative) small perturbations of integrable ones is, in general, the existence of a set of invariant tori which are slightly distorted with respect to the ones pertaining to the unperturbed system. In the typical case, for the perturbed system the set of invariant tori is known to fill a « large part » of phase space, in the sense that the measure of its complement tends to zero with the perturbation. In particular these results have been applied to the classical problem of the heavy rigid body with a fixed point (13) (see also appendix 8 of ref. (9)).

However, a clear understanding of the type of motions which occur for initial data in the set complementary to the set of invariant tori is still lacking. In fact, almost all available information in this connection up to now just comes from numerical computations (see, however, ref. (9,14-19)). The typical case, as has always been confirmed in all examples examined after the first classical numerical investigation of Hénon and Heiles (20), appears to be the following: that for small enough perturbations the computations show only very regular orbits, lying apparently on invariant tori, while for larger perturbations a part of the tori seems to be destroyed, and erratic or chaotic orbits appear instead, filling a so-called stochastic region. These motions starting in the set complementary to the set of invariant tori have indeed in general many properties which pertain to typically chaotic motions, such as that of being visually scattered through some region and that of having positive maximal Ljapunov characteristic exponent (21,22). This phenomenon of the blowing up of the complementary set as perturbation increases has been for this reason described as the occurrence of a « stochastic transition » or, as we prefer to say, of a « transition to stochasticity ». Clearly, the existence of a stochastic region in the above-described sense is not compatible with the integrability of the system.

Now, if one comes to the problem of the heavy rigid body with a fixed point, one can find, to our knowledge, no work which rigorously implies the existence of chaotic motions apart from the very interesting recent works

mathematical Studies, No. 77 (Princeton, 1973).

(16) V. I. ARNOL'D: *Stability problems and the ergodic properties of classical dynamical systems*, in *Proceedings of the 1966 International Congress on Mathematics* (Moscow, 1968, in Russian), p. 387.

(17) N. N. NEKHOROSHEV: *Usp. Mat. Nauk*, **33**, No. 6, 5 (1977, in Russian) (English translation *Russian Math. Surv.*, **33**, No. 6 (1977)).

(18) G. M. ZASLAVSKIJ and B. V. CHIRIKOV: *Usp. Fiz. Nauk*, **105**, No. 1, 3 (1971, in Russian) (English translation *Sov. Phys. Usp.*, **14**, No. 5, 549 (1972)).

(19) G. M. ZASLAVSKIJ: *Statistical Irreversibility in Nonlinear Systems* (Moscow, 1970, in Russian).

(20) M. HÉNON and C. HEILES: *Astron. J.*, **69**, 73 (1964).

(21) G. BENETTIN, L. GALGANI and J.-M. STRELCYN: *Phys. Rev. A*, **14**, 2338 (1976).

(22) G. BENETTIN and J.-M. STRELCYN: *Phys. Rev. A*, **17**, 773 (1978).

of Kozlov and Ziglin⁽²³⁾. Neither we know of works that exhibit the existence of chaotic motions and of a transition to stochasticity in such a problem⁽²⁴⁾ through numerical evidence, although this could be expected according to the above-mentioned general considerations.

The aim of the present paper is indeed to show numerically the existence of chaotic motions and of a transition to stochasticity in the classical problem of the heavy rigid body with a fixed point. More precisely, evidence of this fact is given here in the particular case of perturbations of the Euler-Poinsot case. As a consequence, this gives numerical evidence of the nonintegrability of the classical problem of the heavy rigid body with a fixed point in the general case. In the future we will also investigate, among other problems, perturbations of the Lagrange-Poisson and of the Kovalevskaja cases.

In sect. 2 we recall the results obtained by HÉNON and HEILES⁽²⁰⁾, in order to introduce the reader to the notion of a transition to stochasticity and to explain some concepts to be used in the next sections, such as that of surface of section. In sect. 3 we recall the definition of a set of variables recently introduced by DEPRIT⁽²⁵⁾, which are particularly convenient for studying the problem of a heavy rigid body with a fixed point, as they actually allow the reduction to a problem with two degrees of freedom. Finally, the numerical results establishing the existence of chaotic motions and of a transition to stochasticity in the problem at hand are presented in sect. 4.

We thank DEPRIT (Cincinnati) and KERNER (Paris) for useful discussions.

2. – The transition to stochasticity in the Hénon-Heiles model.

The model considered by HÉNON and HEILES⁽²⁰⁾ consists of two harmonic oscillators of the same frequency coupled by cubic terms in the co-ordinates, as described by the Hamiltonian

$$H(x, y, p_x, p_y) = \frac{1}{2}(p_x^2 + x^2) + \frac{1}{2}(p_y^2 + y^2) + x^2y - \frac{1}{3}y^3,$$

where $x, y, p_x, p_y \in \mathbf{R}$. This model turns out to be of astronomical interest, in connection with studies of galactic motions. Many investigations on models of

⁽²³⁾ V. V. KOZLOV: *Vestn. Mosk. Univ., Mat. Mekh.*, **6**, 99 (1976, in Russian) (English translation *Mosk. Univ. Vestn., Mekh.*, **31**, No. 6, 55 (1976)); *Usp. Mat. Nauk*, **34**, No. 5, 241 (1979, in Russian); S. L. ZIGLIN: *Dokl. Akad. Nauk SSSR*, **251**, No. 4, 786 (1980, in Russian).

⁽²⁴⁾ It might, however, be interesting to note that in the well-known Lorentz system of equations, which is nonconservative, but presents some formal analogies with the Euler equations (with $A = 2$, $B = C = 1$), the existence of a very complex structure of chaotic motions has been numerically observed. See O. LANFORD: in *Statistical Mechanics*, CIME Course, Bressanone, 1976, edited by G. GALLAVOTTI (Napoli, 1978).

⁽²⁵⁾ A. DEPRIT: *Am. J. Phys.*, **55**, 424 (1967).

this type had already been performed by CONTOPOULOS⁽²⁶⁾ with the aim of showing that these systems were « practically integrable ». This was actually shown to occur at least for not too high energies, in the sense that the computed orbits were indeed found to be very regular and one could find phase-space functions which were « practically » integrals of motion. More precisely, one can define formal power series in the variables x, y, p_x, p_y which are practically integrals of motion, in the sense that the fluctuations of the numerically computed values they take along an orbit when the series are truncated at several orders appear to diminish and to become negligible as the order increases (for example, up to order 13)⁽²⁶⁻³⁰⁾.

On the other hand, HÉNON and HEILES discovered that, if energy was raised, chaotic motions came to occur. In order to exhibit this fact, one makes use of the classical tool of the Poincaré surface of section, which consists in considering, instead of a whole orbit in phase space, the sequence of points obtained by its intersection with a suitable fixed submanifold (surface of section). In the Hénon and Heiles experiment the sequence of points is obtained as follows. Consider a surface of constant energy E . For $0 < E < \frac{1}{6}$ it contains a unique compact component which we denote as Γ_E . Taking in Γ_E the two-dimensional surface given by $x = 0$, one considers the successive points at which a particular solution intersects this two-dimensional surface with $p_x > 0$. If one eliminates p_x with the help of $H = E$ and sets $x = 0$, one can use y and p_y as co-ordinates on this two-dimensional surface and thus one can plot the points of intersection on the plane region:

$$\tilde{\Gamma}_E = \{(y, p_y) \in \mathbf{R}^2; \frac{1}{2}(p_y^2 + y^2) - \frac{1}{3}y^3 \leq E, y \leq 1\}.$$

Now we can describe the transition to stochasticity by making reference to fig. 1-3. One considers several initial data on a fixed energy surface Γ_E and each of the corresponding orbits defines a sequence of points in $\tilde{\Gamma}_E$ as above. A first example, corresponding to $E = \frac{1}{12}$, is given in fig. 1. Several orbits have been computed here, and for each of them the corresponding points appear to lie on a very regular closed curve; any such curve would be densely filled if the orbits were computed for longer and longer times. Moreover, the set of such regular curves appears to practically cover all of $\tilde{\Gamma}_E$.

The opposite situation occurs, for example, for $E = \frac{1}{6}$, shown by fig. 2. Here five orbits have been computed and for one of them the corresponding points in $\tilde{\Gamma}_E$ appear visually to almost densely fill all of it. In fact, just a small

⁽²⁶⁾ G. CONTOPOULOS: *Astron. J.*, **68**, 3 (1963).

⁽²⁷⁾ F. GUSTAVSON: *Astron. J.*, **71**, 670 (1966).

⁽²⁸⁾ A. GIORGILLI and L. GALGANI: *Cel. Mech.*, **17**, 267 (1978).

⁽²⁹⁾ A. GIORGILLI: *Comput. Phys. Commun.*, **16**, 331 (1979).

⁽³⁰⁾ G. GONTOPOULOS, L. GALGANI and A. GIORGILLI: *Phys. Rev. A*, **18**, 1183 (1978).

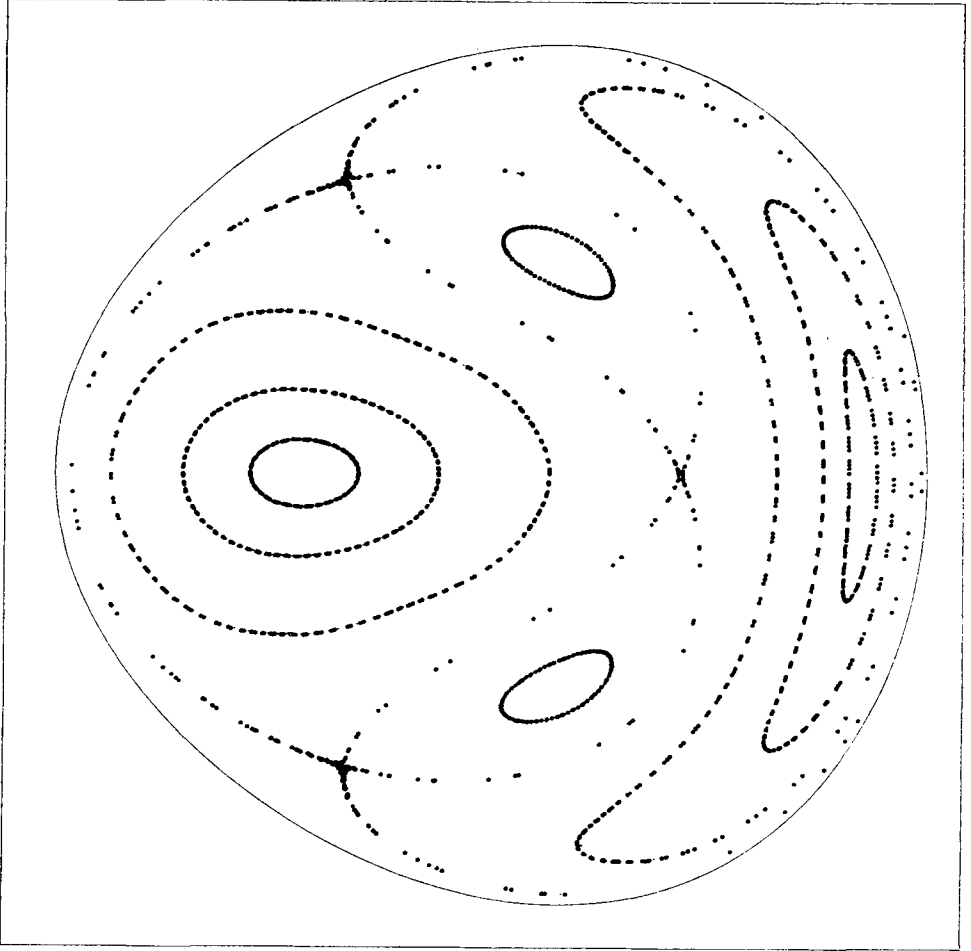


Fig. 1. — Surface of section for the Hénon-Heiles model when the energy has value $E = 1/12$. This figure shows a typical practically-integrable situation.

part of $\tilde{\Gamma}_E$, for example around the centre of the figure, appears to be covered by regular curves.

In general, for intermediate values of the energy, $\tilde{\Gamma}_E$ appears to be subdivided into two invariant sets. One of these seems to be covered by regular closed curves and the other one by sequences of scattered points with a visual chaotic behaviour, each sequence corresponding to an individual chaotic orbit. This situation is illustrated by fig. 3, which refers to $E = \frac{1}{3}$, where one chaotic orbit is visualized.

The qualitative differences between the region apparently covered by regular curves, which can be called the « ordered region », and the other region which can be called stochastic or chaotic, are striking. Possibly one of the

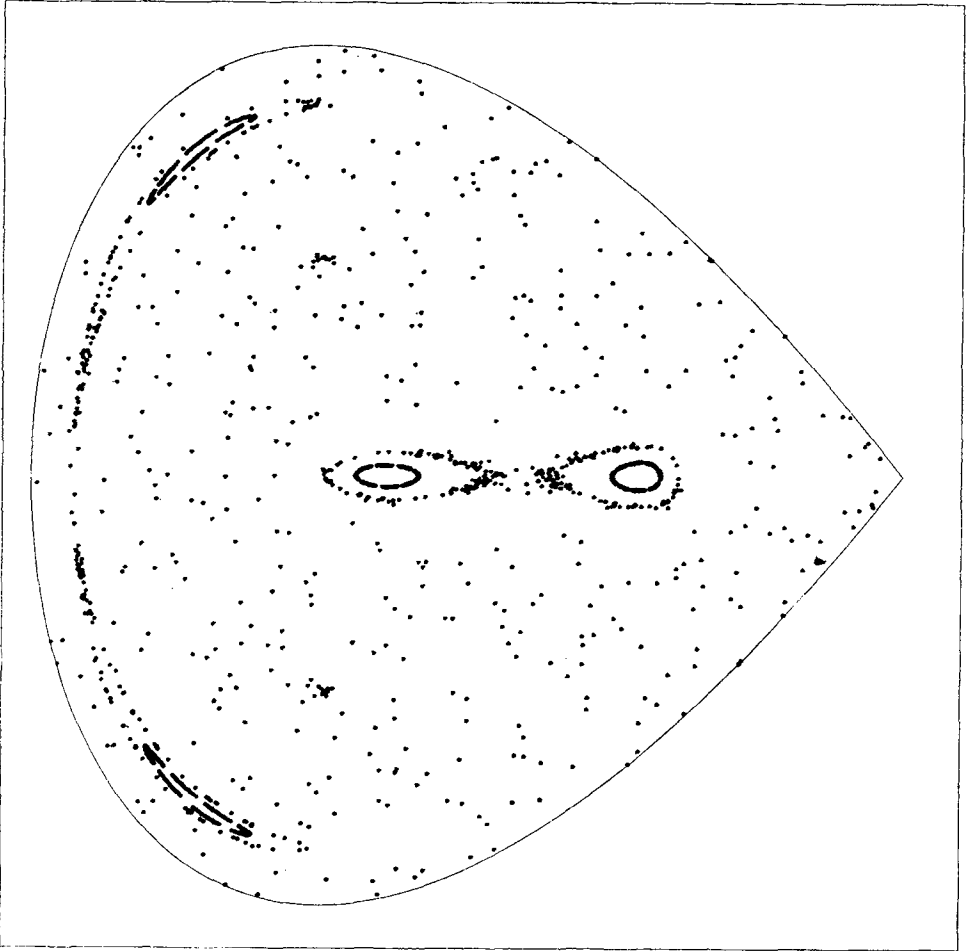


Fig. 2. — Same as fig. 1 for $E = 1/6$, showing a typical almost completely chaotic situation.

main features distinguishing these regions is the following: motions have a predictable character in the ordered region and an unpredictable one in the stochastic region. This is strictly related to the way in which the orbits depend on the initial data; indeed the computations show that orbits with nearby initial data diverge from each other exponentially with time in the stochastic region and in a substantially slower way in the ordered region.

This circumstance, in turn, can be formalized by making reference to the maximal Ljapunov characteristic exponent (LCE) of an orbit. A numerical method to compute the maximal LCE is described in ref. ⁽²¹⁾, where an application to the Hénon-Heiles model is also given; a minor technical improvement, as well as a general numerical algorithm to compute all LCEs, is

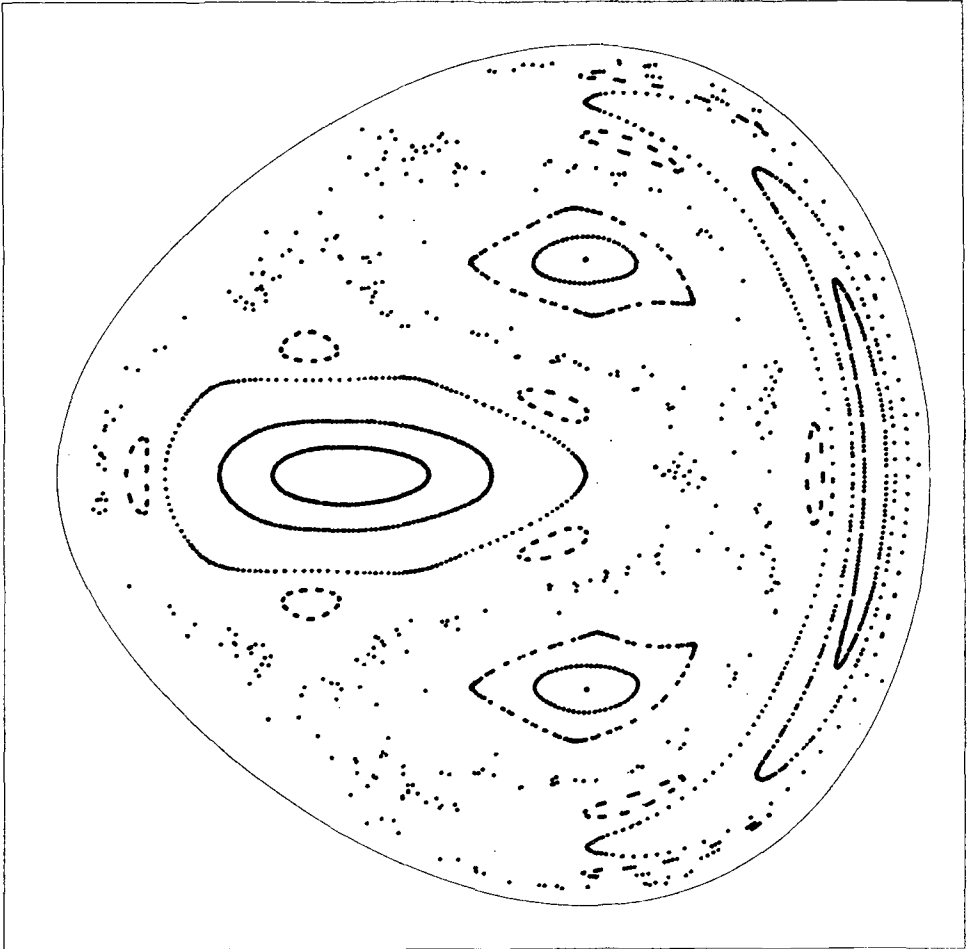


Fig. 3. - Same as fig. 1 for $E=1/8$, showing a typical intermediate situation.

given in ref. ⁽³¹⁾. It can be proven that the maximal LCE vanishes almost everywhere for integrable systems; several numerical computations ^(21,22,32) show instead that it vanishes in the ordered region, while it appears to be definitely positive in the stochastic region.

⁽³¹⁾ G. BENETTIN, L. GALGANI, A. GIORGILLI and J.-M. STRELCYN: *Meccanica*, **15**, 9, 21 (1980). See also G. BENETTIN, L. GALGANI, A. GIORGILLI and J.-M. STRELCYN: *C. R. Acad. Sci. Ser. A*, **286**, 431 (1978); G. BENETTIN and L. GALGANI: *Ljapunov characteristic exponents and stochasticity*, in *Intrins. Stochast. in Plasma, Cargese* (1979, in print).

⁽³²⁾ V. I. OSELEDEC: *Tr. Mosk. Mat. Obsch.* **19**, 179 (1968, in Russian) (English translation *Trans. Mosc. Math. Soc.*, **19**, 197 (1968)).

3. – The Deprit variables in the problem of the rigid body with a fixed point.

The Hamiltonian and the corresponding equations of motion for a rigid body with a fixed point take a form much simpler than the usual one related to the Euler angles and the corresponding momenta, if one makes reference to a set of variables which were introduced quite recently in this connection by DEPRIT⁽²⁵⁾, although they can also be found, in connection with the problem of celestial mechanics, in an older textbook of ANDOYER⁽²³⁾; a systematic use of such variables in the problem at hand is made in the recent book of Arhangelskij⁽⁸⁾.

Let us, as usual, take the fixed point O around which the body is rotating as the origin of two right-hand orthogonal co-ordinate frames: the frame $OXYZ$ fixed in space with the Z -axis vertical and the moving frame $Oxyz$ which is fixed relative to the body. The corresponding unit vectors are denoted as usual by $\mathbf{I}, \mathbf{J}, \mathbf{K}$ and $\mathbf{i}, \mathbf{j}, \mathbf{k}$, respectively. The axes of the moving frames are directed along the principal axes of inertia of the body, and the corresponding principal moments of inertia (which we will suppose to be strictly positive) are denoted by A, B and C , respectively. Let $\mathbf{\Gamma}$ be the angular momentum of the body with respect to O and Π the plane through O normal to $\mathbf{\Gamma}$. If \mathbf{k}, \mathbf{K} and $\mathbf{\Gamma}$ are distinct, the plane Π cuts the plane OXY along a straight line OM and the plane Oxy along a straight line ON , which we orient as $\mathbf{K} \wedge \mathbf{\Gamma}$ and $\mathbf{\Gamma} \wedge \mathbf{k}$, respectively.

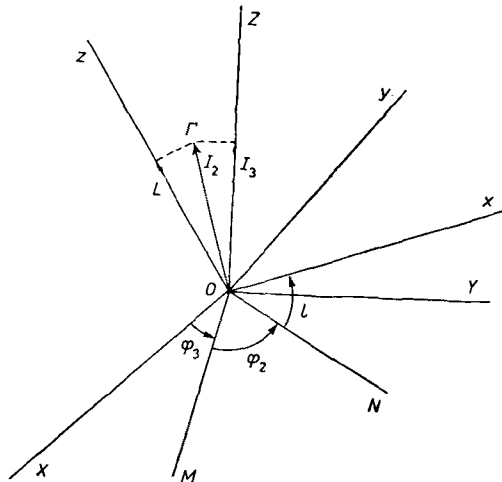


Fig. 4. – The Deprit angles.

(23) H. ANDOYER: *Cours de mécanique celeste* (Paris, 1923).

The Deprit angles φ_3, φ_2, l with $0 \leq \varphi_3 < 2\pi, 0 \leq \varphi_2 < 2\pi, 0 \leq l < 2\pi$ are then defined as in fig. 4, *i.e.* φ_3 is the longitude of the plane Π in the co-ordinate plane OXY , φ_2 is the longitude with respect to OM of the plane (of inertia) Oxy in the plane Π and l is the angle of rotation of the axis of inertia Ox with respect to the intersection ON of the plane of inertia Oxy with the plane Π . The corresponding momenta I_3, I_2, L are defined through suitable components of the angular momentum $\mathbf{\Gamma}$, namely $I_3 = \Gamma_z, I_2 = \Gamma, L = \Gamma_z$, respectively, where $\Gamma_z = \mathbf{\Gamma} \cdot \mathbf{K}, \Gamma_z = \mathbf{\Gamma} \cdot \mathbf{k}$, and Γ is the norm of $\mathbf{\Gamma}$.

If φ, θ, ψ are the usual Euler angles and $p_\varphi, p_\theta, p_\psi$ the corresponding momenta, one easily shows that the transformation $(\varphi, \theta, \psi, p_\varphi, p_\theta, p_\psi) \mapsto (\varphi_3, \varphi_2, l, I_3, I_2, L)$ is canonical. The notations for the Deprit variables used here are taken from Arhangelskij's book ⁽⁸⁾, whose choice reflects the fact that $I_3, I_2, \varphi_3, \varphi_2$ are already action-angle variables for the Euler-Poinsot case.

The problem is now to express the Hamiltonian H in the Deprit variables. Let us start with the Euler-Poinsot case when $H = H_0 = T$, where T is the kinetic energy. Recall that

$$(1) \quad T = \frac{1}{2} \left(\frac{I_x^2}{A} + \frac{I_y^2}{B} + \frac{I_z^2}{C} \right),$$

where I_x, I_y, I_z are the components of $\mathbf{\Gamma}$ in the frame $Oxyz$. We already have $I_z = L$. Denote now by $\mathbf{\Gamma}_{xy}$ the projection of $\mathbf{\Gamma}$ on the plane Oxy and by Γ_{xy} its norm. One easily sees that

$$\Gamma_{xy} = \sqrt{I_2^2 - L^2}, \quad I_x = \Gamma_{xy} \sin l, \quad I_y = \Gamma_{xy} \cos l,$$

so that one gets

$$(2) \quad H_0 = \frac{I_2^2 - L^2}{2} \left(\frac{\sin^2 l}{A} + \frac{\cos^2 l}{B} \right) + \frac{L^2}{2C}.$$

Let us now pause to comment on formula (2), which is the Hamiltonian for the Euler-Poinsot case in the Deprit variables. As one sees, the variables $\varphi_3, \varphi_2, I_3$ do not appear there. From the Hamilton equations one thus gets that the variables $\varphi_3, I_3 = \Gamma_z$ and $I_2 = \Gamma$ are constant, as was already clear from conservation of angular momentum. Denoting $I_2 = \alpha = \text{const}$, the problem is then reduced to that of a conservative system with one degree of freedom with variables l, L and Hamiltonian

$$(3) \quad H_\alpha(l, L) = \frac{\alpha^2 - L^2}{2} \left(\frac{\sin^2 l}{A} + \frac{\cos^2 l}{B} \right) + \frac{L^2}{2C}.$$

Thus, through the Deprit variables, the Euler-Poinsot problem can be treated as the familiar conservative one-dimensional problems, such as typically the

plane pendulum. Indeed, for a fixed α , in the phase (l, L) -plane one has just to trace the level curves $\gamma_{E,\alpha}$ of H_α to obtain the projection of phase-space trajectories; these cover the rectangle $\{(l, L); 0 \leq l < 2\pi, -\alpha \leq L \leq \alpha\}$. each one corresponding to a particular value of E .

However, for the perturbation of Hamiltonian (2) we will be interested in the study of surfaces of section of the corresponding flow at a fixed energy E , in analogy with the description given in sect. 2; thus it is more convenient for us, even for the unperturbed Hamiltonian (2), to consider another representation. Namely, instead of a fixed value of α we take a fixed value of the energy E and we obtain phase-space trajectories whose projection in the (l, L) -plane are level curves $\gamma_{E,\alpha}$ of Hamiltonian (3), each corresponding to a

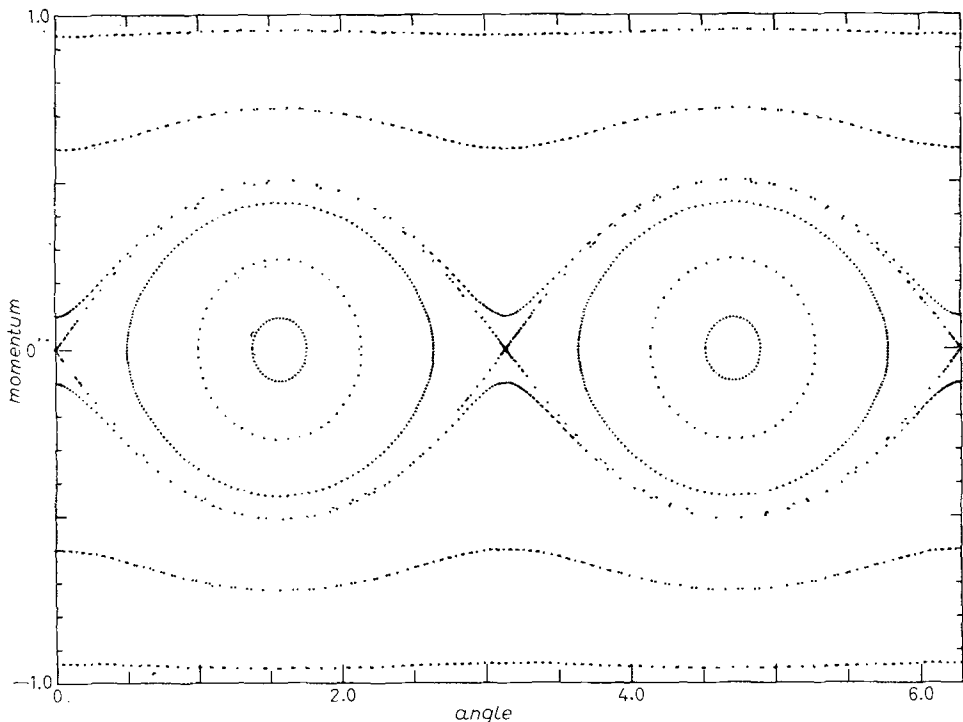


Fig. 5. - The integrable case of the rigid body with a fixed point and no weight, described by the Hamiltonian (2) with two degrees of freedom, co-ordinates l and φ_2 , momenta L and I_2 . As φ_2 is ignorable and thus $I_2 = \alpha = \text{const}$, the problem is essentially one-dimensional and the projections of the phase-space trajectories on the (l, L) -plane coincide with the level curves of Hamiltonian (3). In the figure one has L/I_2 vs. l for several values of α and a fixed value of the energy $E = 50$ with $A = 3$, $B = 2$, $C = 1$. Actually, the points have been obtained by integrating the Hamiltonian equations for Hamiltonian (2) and by taking as surface of section the one defined by $\varphi_2 = (\pi/2) \pmod{2\pi}$, in complete analogy with the methods used in the perturbed cases of fig. 7-13.

particular value of $\alpha = I_2$. It is easily seen (as one always has $\alpha \geq |L|$) that these curves cover the rectangle $\{(l, L); 0 \leq l < 2\pi, |L| \leq \alpha_E\}$, where $\alpha_E = \sqrt{2EC}$. Using as co-ordinates l and $L/I_2 = \Gamma_z/\Gamma$ instead of l and L , the curves cover a rectangle which is independent of E , namely $\{(l, L/I_2); 0 \leq l < 2\pi, -1 \leq L/I_2 \leq 1\}$. As an example we report in fig. 5 some phase-space trajectories $\gamma_{E,\alpha}$ for $A = 3, B = 2, C = 1$ and $E = 50$, which are just the values which will also be considered by us in the perturbed case.

The qualitative features of fig. 5 are easily understood if one recalls the well-known consideration which gives the possible positions of $\mathbf{\Gamma}$ with respect to the moving frame $Oxyz$ (see ref. (9), sect. 29). Indeed, due to conservation of energy E and of angular momentum $\mathbf{\Gamma}$ one has

$$\frac{\Gamma_x^2}{A^2} + \frac{\Gamma_y^2}{B^2} + \frac{\Gamma_z^2}{C^2} = 2E = \text{const}, \quad I_x^2 + I_y^2 + I_z^2 = I^2 = \text{const},$$

so that the vector $\mathbf{\Gamma}$ lies on the intersection of an ellipsoid with a sphere both fixed with the body. The curves traced by $\mathbf{\Gamma}$ on the ellipsoid are easily recognized to be qualitatively of the form reproduced in fig. 6, which refers to a case with $A > B > C > 0$. If we take into account that $L = \Gamma_z$ and the definition of l (see fig. 4), the qualitative features of fig. 5 then follow.

One easily thus recognizes that the two fixed points at $(\pi/2, 0), (3\pi/2, 0)$ correspond to the stable permanent rotations about the axis Ox , the two fixed

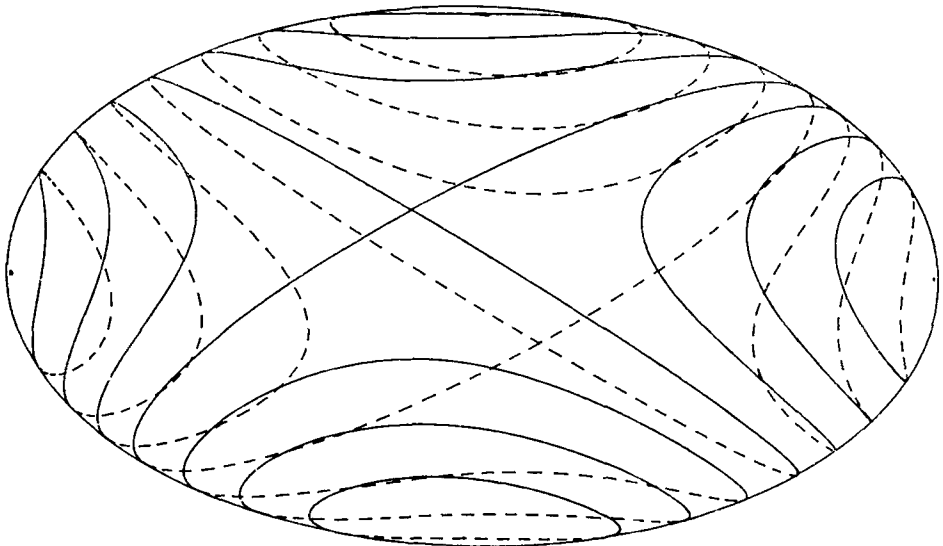


Fig. 6. - It explains the qualitative features of fig. 5 and shows possible positions of the angular momentum $\mathbf{\Gamma}$ with respect to the moving frame for a fixed value of the energy. The various curves correspond to different values of the norm of $\mathbf{\Gamma}$.

points at $(0, 0)$ and $(\pi, 0)$ to the unstable permanent rotations about the axis Oy and the straight lines $L/I_2 = -1$, $L/I_2 = 1$ to the stable permanent rotations about the axis Oz . Notice that in the latter case the plane of inertia Oxy coincides at all times with the «invariable» plane II , so that the rotation angle l is no longer determined; thus the periodic orbits $L/I_2 = -1$ and $L/I_2 = 1$ in the phase plane l , L/I_2 can be considered as fixed points too. The separatrices connecting the two unstable fixed points are also exhibited.

Finally, let us come to the case in which gravity is taken into consideration. Let x_0, y_0, z_0 denote the co-ordinates of the centre of mass in the moving frame $Oxyz$, let Z_0 be its third co-ordinate in the fixed frame $OXYZ$ and define $\gamma = \mathbf{i} \cdot \mathbf{K}$, $\gamma' = \mathbf{j} \cdot \mathbf{K}$, $\gamma'' = \mathbf{k} \cdot \mathbf{K}$. Then one has $H = H_0 + mgZ_0$, *i.e.*

$$(4) \quad H = H_0 + mg(x_0\gamma + y_0\gamma' + z_0\gamma''),$$

where m and g are the mass of the body and the acceleration of gravity, respectively. The rather complicated expressions for $\gamma, \gamma', \gamma''$ in terms of the Deprit variables can be found for example at page 22 of ref. (8) and are given by

$$(5) \quad \left\{ \begin{array}{l} \gamma = \frac{I_3}{I_2} \left(1 - \frac{L}{I_2}\right)^{\frac{1}{2}} \sin l + \left(1 - \frac{I_3^2}{I_2^2}\right)^{\frac{1}{2}} \frac{L}{I_2} \sin l \cos \varphi_2 + \left(1 - \frac{I_3^2}{I_2^2}\right)^{\frac{1}{2}} \cos l \sin \varphi_2, \\ \gamma' = \frac{I_3}{I_2} \left(1 - \frac{L}{I_2}\right)^{\frac{1}{2}} \cos l + \left(1 - \frac{I_3^2}{I_2^2}\right)^{\frac{1}{2}} \frac{L}{I_2} \cos l \cos \varphi_2 - \left(1 - \frac{I_3^2}{I_2^2}\right)^{\frac{1}{2}} \sin l \sin \varphi_2, \\ \gamma'' = \frac{I_3 L}{I_2^2} - \left(1 - \frac{I_3^2}{I_2^2}\right)^{\frac{1}{2}} \left(1 - \frac{L^2}{I_2^2}\right)^{\frac{1}{2}} \cos \varphi_2. \end{array} \right.$$

As we already know that $I_3 = \Gamma_z$ is an integral of motion and that $I_2 = \Gamma \geq |I_3|$, if we take $I_3 = \beta \neq 0$, then we have $I_2 \geq |\beta| > 0$, and no problem arises in the expressions of (5). Hamiltonian (4) refers to a system with three degrees of freedom. For the purposes of this paper it is sufficient to consider, in fact, the corresponding one-parameter family of Hamiltonians with two degrees of freedom which is obtained by putting $I_3 = \beta \neq 0$ in (4). To this we will refer from now on.

Fix $\beta \neq 0$. Denote by $\Gamma_{E,\beta}$ the constant-energy surface corresponding to an energy E , whose possible range is $-mg(x_0^2 + y_0^2 + z_0^2)^{\frac{1}{2}} \leq E < \infty$. It is easy to see that $\Gamma_{E,\beta}$ is always compact. Indeed, as φ_2 and l are defined modulo 2π and we already know that $|I_3| \leq I_2$ and that $|L| \leq I_2$, then it is sufficient to show that I_2 is uniformly bounded from above when $(\varphi_2, l, I_2, L) \in \Gamma_{E,\beta}$. In turn, this follows from the remark that $T = E - mgZ_0$ is uniformly bounded from above (as $|Z_0| \leq \sqrt{x_0^2 + y_0^2 + z_0^2}$), which by (1) implies the same for $|\Gamma_x|, |\Gamma_y|, |\Gamma_z|$ and thus also for $I_2 = \Gamma$.

Actually, a sufficient generality for the qualitative purposes of our investigation is afforded even if we take the centre of mass on the axis Oz , *i.e.* if we put

$x_0 = y_0 = 0$ in Hamiltonian (4). From (5) one thus gets

$$(6) \quad H(\varphi_2, l, I_2, L; \mu, \beta) = \frac{I_2^2 - L^2}{2} \left(\frac{\sin^2 l}{A} + \frac{\cos^2 l}{B} \right) + \frac{L^2}{2C} + \\ + \mu \left[\frac{\beta L}{I_2^2} - \left(1 - \frac{\beta^2}{I_2^2} \right)^{\frac{1}{2}} \left(1 - \frac{L^2}{I_2^2} \right)^{\frac{1}{2}} \cos \varphi_2 \right],$$

where $\mu = mgz_0$ and $\beta \neq 0$ is the constant value of $I_3 = I_z$.

Notice that the Hamiltonian (6), as well as H_0 , is a periodic function of l with period π , while the period is 2π for the complete Hamiltonian (4). As a consequence, it is easy to see that, if $\{\varphi_2(t), l(t), I_2(t), L(t)\}_{t \in \mathbb{R}}$ is a solution of the equations of motion for Hamiltonian (6), then $\{\varphi_2(t), l(t) + \pi, I_2(t), L(t)\}_{t \in \mathbb{R}}$ is also a solution.

4. - Results of numerical computations.

Our aim is thus to integrate numerically the equations of motion for Hamiltonian (6) and to produce figures analogous to fig. 1-3 in order to exhibit the occurrence of chaotic motions and of a transition to stochasticity as $\mu \geq 0$ is increased.

All computations were performed for $A = 3$, $B = 2$, $C = 1$, $\beta = I_3 = I_z = 5$, $E = 50$ with μ taking values in the interval 0.40, precisely $\mu = 0, 0.1, 0.5, 1, 5, 10, 20, 30$. The computations were performed on a PDP11 with a precision of 7 digits, by using a standard Runge-Kutta fourth-order method with time step typically of 0.01; this guaranteed energy conservation up to 4 digits for times sufficient to give typically 1000 points of section. For questions concerning the reliability of numerical computations in the study of stochasticity, see ref. (34).

As is well known (see for example sect. 28D of ref. (9)), having chosen a model with $A = B + C$ we are necessarily considering a plane rigid body. An example of a rigid body satisfying our conditions $A = 3$, $B = 2$, $C = 1$ is the one constituted by four material points of unitary mass at the vertices of a unit square, the fixed point 0 lying in the middle of one of its sides.

After having fixed values of μ , β and E , the initial data were obtained by giving certain values to l and L , by taking $\varphi_2 = \pi/2$ and getting $I_2 > 0$ from the equation $H(\pi/2, l, I_2, L; \mu, \beta) = E$. In all cases considered it turned out that this equation had one and two positive solutions for $L < 0$ and $L > 0$, respectively; moreover in the latter situation only the maximal solution had a mechanical meaning, namely satisfied the necessary conditions $I_2 \geq |L|$, $I_2 \geq |\beta|$.

(34) G. BENETTIN, M. CASARTELLI, L. GALGANI, A. GIORGILLI and J.-M. STRELCYN: *Nuovo Cimento B*, **44**, 183 (1978); **50**, 211 (1979).

Our surface of section in $\Gamma_{E,\beta}$ was also defined by the condition $\varphi_2 = (\pi/2) \pmod{2\pi}$. Given a trajectory in phase space, the condition $\varphi_2 = (\pi/2) \pmod{2\pi}$ defines a sequence of points, representing the trajectory on the surface of section. In full analogy with the treatment of the unperturbed problem, each point of this sequence can then be represented as a point in the plane \mathbf{R}^2 through two co-ordinates l and L/I_2 , I_2 being a well-defined function of l and L . Thus to any trajectory there corresponds a sequence of points in the rectangle $\tilde{F} = \{(l, L/I_2); 0 \leq l < 2p, -1 < L/I_2 < 1\}$. This choice of L/I_2 instead of L as a co-ordinate, notwithstanding the fact that I_2 is not an integral of motion for $\mu \neq 0$, has the advantage that the corresponding region \tilde{F} has then a very simple form; on the other hand the possibility of recognizing the regular or chaotic character of an orbit is not affected by that choice, due to the fact that $\Gamma_{E,\beta}$ is compact and I_2 is a strictly positive smooth function defined on $\Gamma_{E,\beta}$.

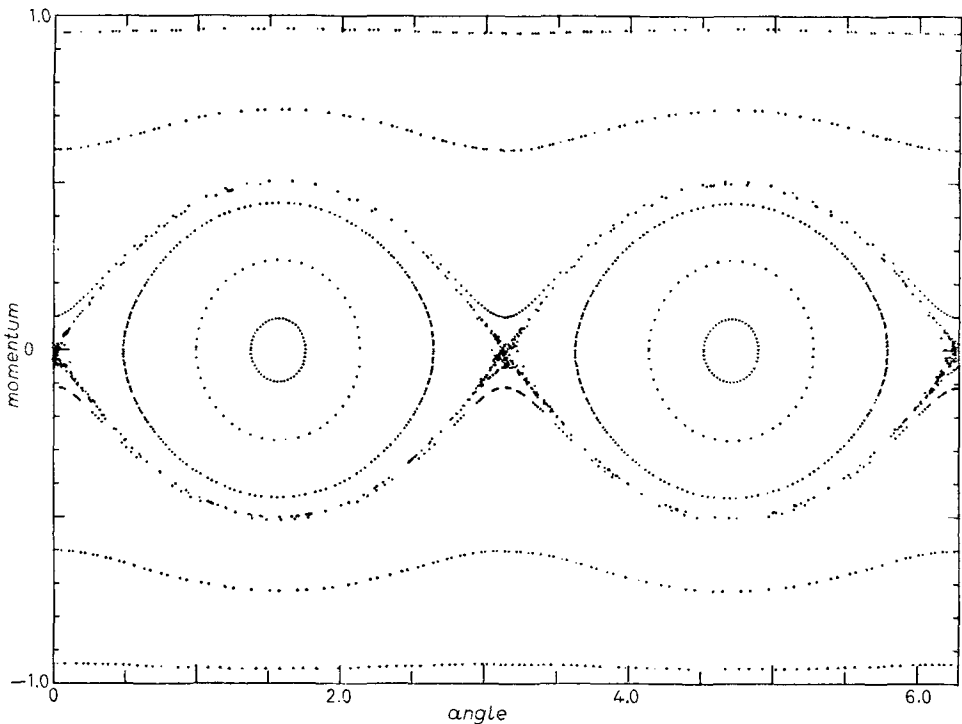


Fig. 7. - From the present figure up to fig. 13 the results are given illustrating the transition to stochasticity in the problem of the heavy rigid body with a fixed point, described by Hamiltonian (6), as the perturbation parameter μ is raised, the values of the other parameters being $A = 3$, $B = 2$, $C = 1$, $E = 50$, $\beta = 5$. The equations of motion have been solved numerically to obtain the points intersecting the surface with $\varphi_2 = (\pi/2) \pmod{2\pi}$ and for them L/I_2 has been plotted *vs.* l , as in fig. 5, which correspond to the unperturbed case with $\mu = 0$. Here $\mu = 0.1$.

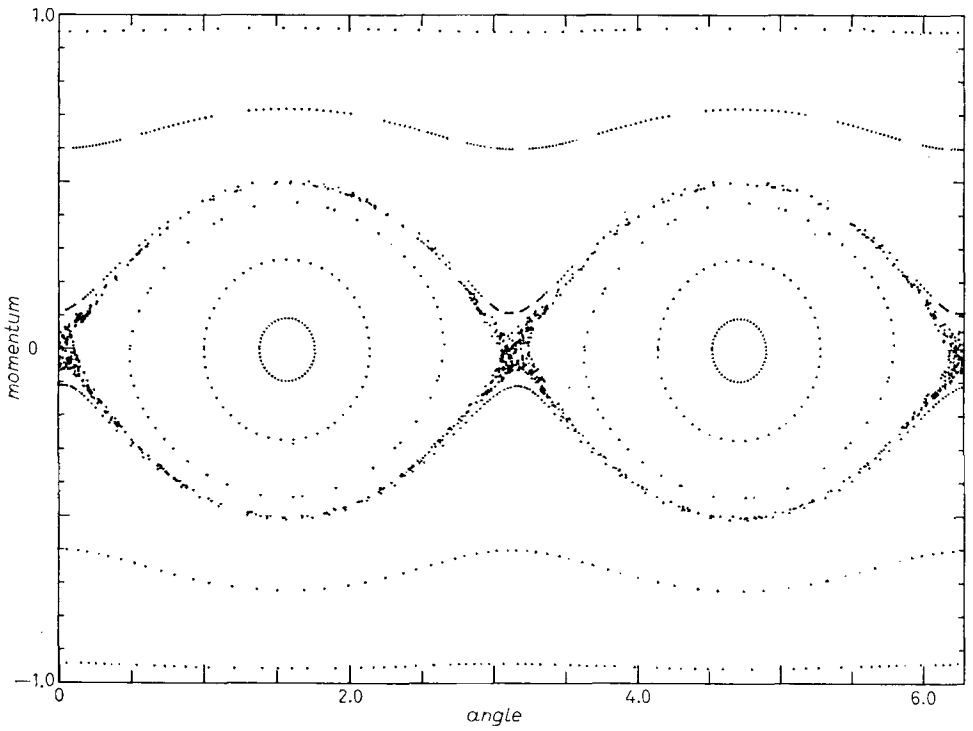


Fig. 8. - Same as fig. 7 with $\mu = 0.5$.

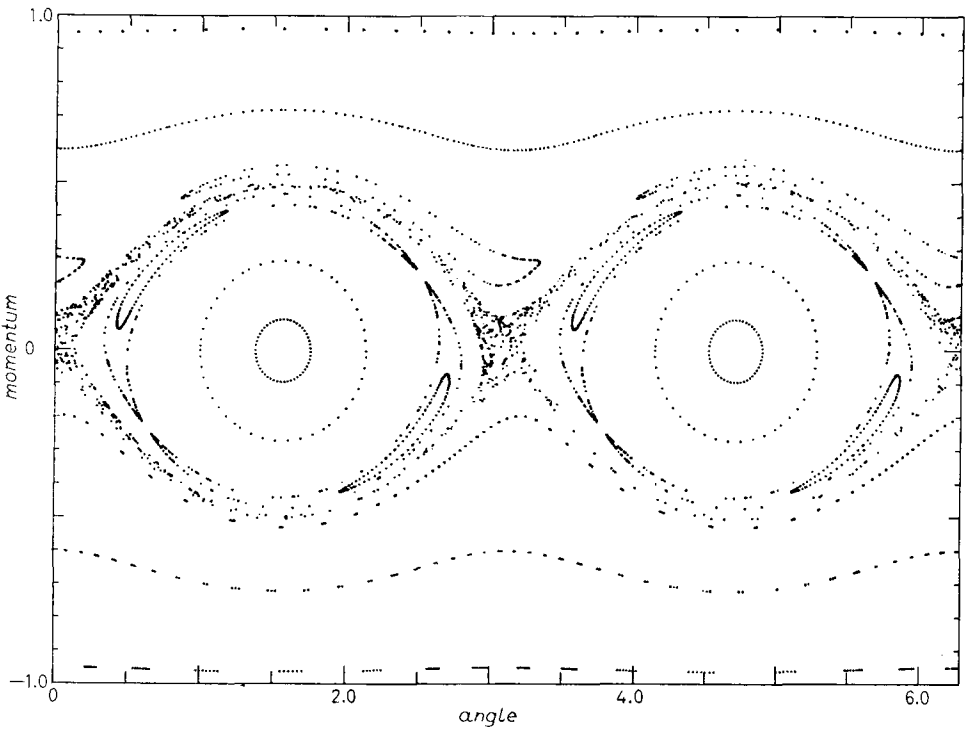


Fig. 9. - Same as fig. 7 with $\mu = 1$.

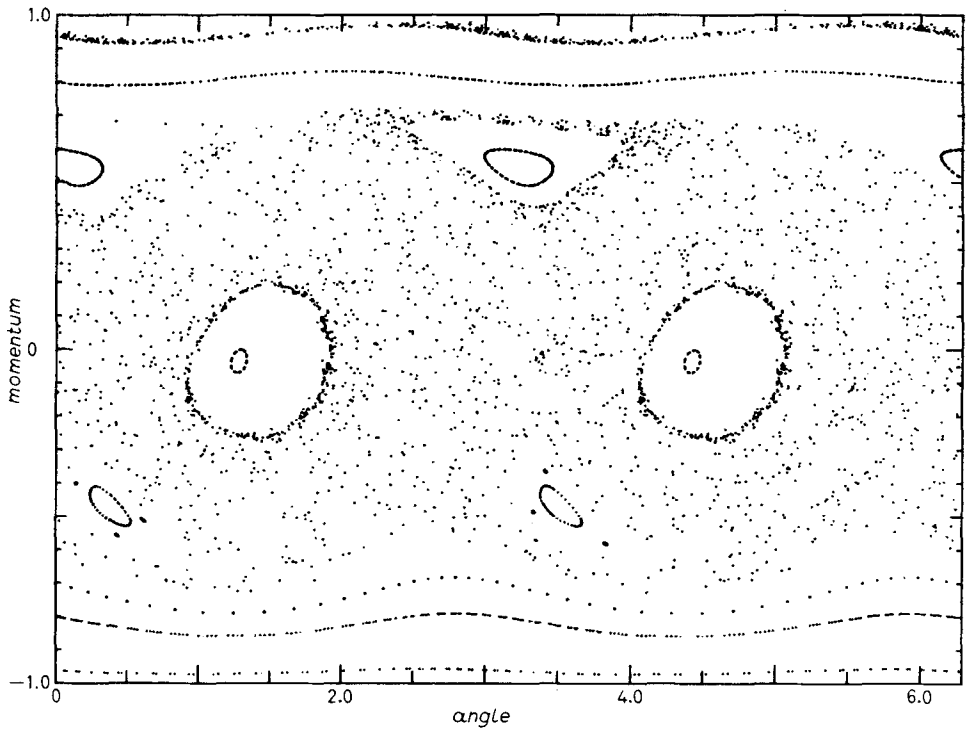


Fig. 12. - Same as fig. 7 with $\mu = 20$.

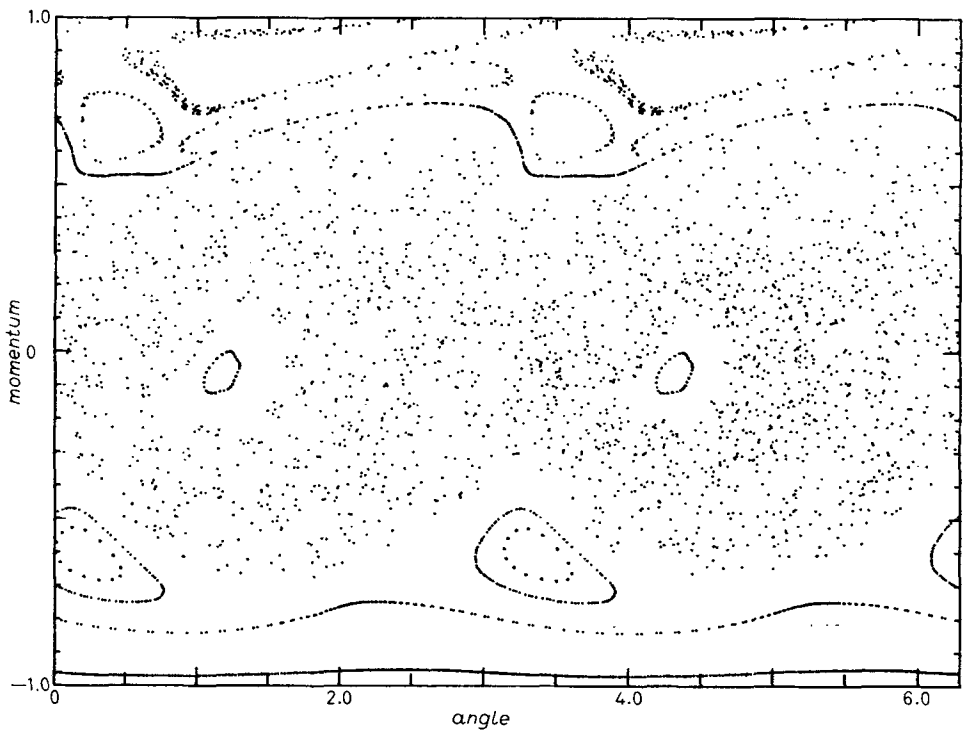


Fig. 13. - Same as fig. 7 with $\mu = 30$.

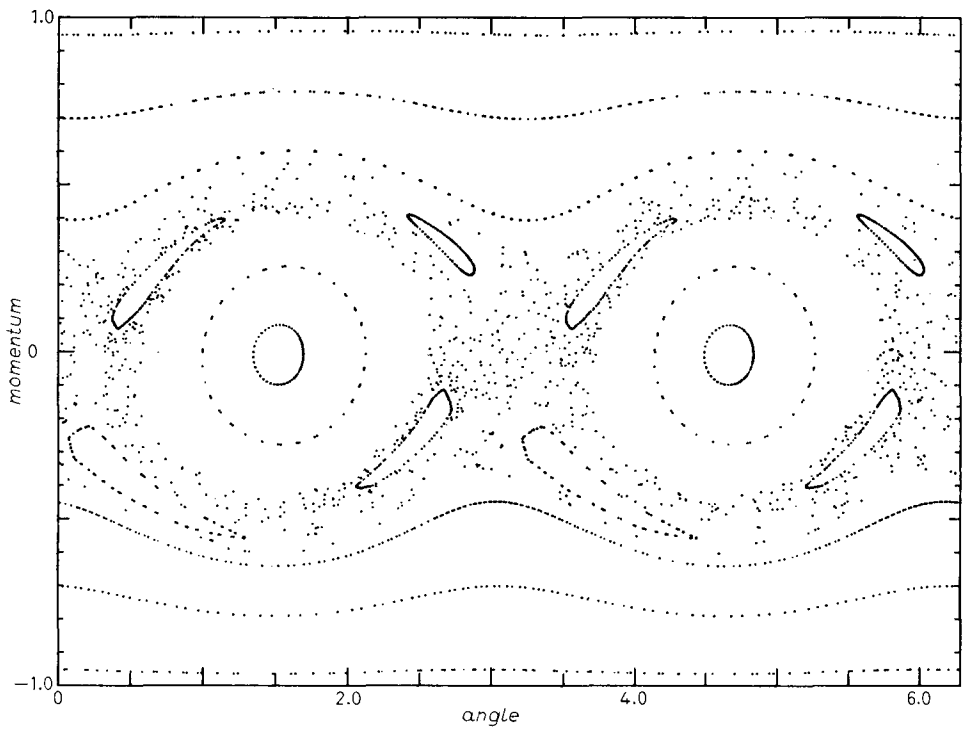


Fig. 10. - Same as fig. 7 with $\mu = 5$.

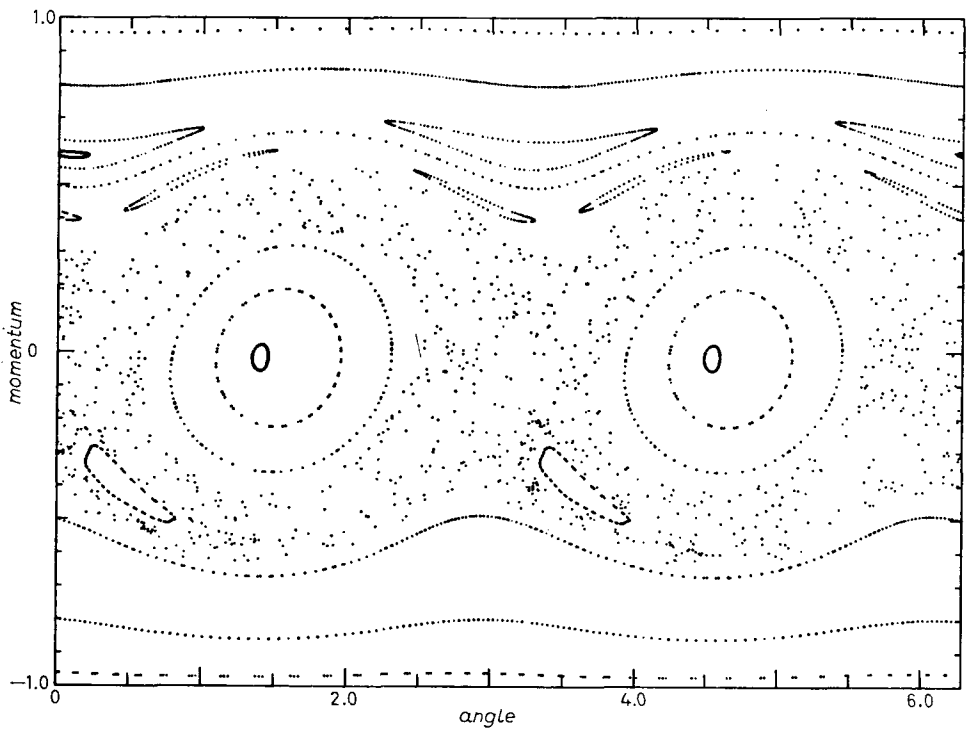


Fig. 11. - Same as fig. 7 with $\mu = 10$.

Let us now come to a description of the results. For $\mu = 0$ the already known results are given in fig. 5. This figure could have been obtained by tracing level curves for the corresponding Hamiltonian (3), but was instead obtained by the above-described method. Figure 7-13 correspond to $\mu = 0.1, 0.5, 1, 5, 10, 20, 30$, respectively.

For $\mu = 0.1$ one already observes a very small stochastic region around the curves which are the separatrices connecting the two unstable fixed points for $\mu = 0$. For $\mu = 0.5$ the situation is similar and just the stochastic region is a bit larger. For $\mu = 1$ a substantial change occurs in the form of the closed curves around the central stable fixed points, inasmuch as islands of higher order appear, while the stochastic region keeps essentially the same form as before being slightly enlarged. Analogously for $\mu = 5$. The process of dissolution of the invariant curves and the corresponding extension of the stochastic region continues when μ is increased from 10 to 30, when the stochastic region occupies the largest part of the available region, *i.e.* of the rectangle \tilde{I} .

As to all fig. 7-13, one sees that the straight line $l = \pi$ divides each of them into two strips, the right one being obtained from the other one by a translation. This is in complete agreement with the last remark of sect. 3.

5. - Conclusions.

We have thus given a numerical evidence for the existence of chaotic motions and of a transition to stochasticity in the classical problem of the heavy rigid body with a fixed point, by studying a convenient perturbation of the Euler-Poinsot case. This, in particular, gives also numerical evidence for the nonintegrability of the classical problem of the heavy rigid body with a fixed point in the general case.

Preliminary investigations of perturbations of the Lagrange-Poisson and of the Kovalevskaja cases appear to confirm the results reported here for perturbations of the Euler-Poinsot case.

Note added in proofs.

There recently appeared a book by V. V. KOZLOV: *Methods of Qualitative Analysis in the Dynamics of Rigid Body* (Moscow, 1980), which is of great interest for the problems considered in the present paper.

● RIASSUNTO

In questo lavoro si mostra numericamente l'esistenza di moti caotici e di una transizione alla stocasticità nel problema classico del corpo rigido pesante con un punto fisso, studiando una perturbazione del caso di Eulero-Poinsot. In tal modo si dà anche una dimostrazione numerica della non integrabilità di questo problema.

Хаотические движения и переход к стохастичности в классической проблеме тяжелого жесткого тела с фиксированной точкой.

Резюме (*). — Мы приводим численное подтверждение существования хаотических движений и перехода к стохастичности в классической проблеме тяжелого жесткого тела с фиксированной точкой, исследуя возмущение для случая Эйлера-Пуансо. Также приводится численное подтверждение для неинтегрируемости такой проблемы.

(*) *Переведено редакцией.*